Rom J Morphol Embryol 2022, 63(2):357–367 ISSN (print) 1220–0522, ISSN (online) 2066–8279 doi: 10.47162/RJME.63.2.07

ORIGINAL PAPER

RJME Romanian Journal of Morphology & Embryology http://www.rjme.ro/

Analysis of the relationship between placental histopathological aspects of preterm and term birth

IOANA VICTORIA CAMEN[1)], ANCA-MARIA ISTRATE-OFIŢERU[2–4)], LILIANA VICTORIA NOVAC[5)], MARIA MAGDALENA MANOLEA[5)], ANDA LORENA DIJMĂRESCU[5)], SIMONA DANIELA NEAMŢU[6)], LUCREŢIU RADU[7)], MIHAIL VIRGIL BOLDEANU[8)], MIRCEA-SEBASTIAN ŞERBĂNESCU[9)], MARIA STOICA[10)], ANDREI GHEORGHE MARIUS MOTOC[11)], MARIUS BOGDAN NOVAC[10)], DANIELA-LOREDANA BUJORESCU[12)]

[1)]*PhD Student, Doctoral School, University of Medicine and Pharmacy of Craiova, Romania*

[2)]*Department of Histology, University of Medicine and Pharmacy of Craiova, Romania*

[3)]*Research Center for Microscopic Morphology and Immunology, University of Medicine and Pharmacy of Craiova, Romania*

[4)]*Department of Obstetrics and Gynecology, Emergency County Hospital, Craiova, Romania*

[5)]*Department of Obstetrics and Gynecology, University of Medicine and Pharmacy of Craiova, Romania*

[6)]*Department of Hematology and Immunology, University of Medicine and Pharmacy of Craiova, Romania*

[7)]*Department of Hygiene, University of Medicine and Pharmacy of Craiova, Romania*

[8)]*Department of Immunology, University of Medicine and Pharmacy of Craiova, Romania*

[9)]*Department of Medical Informatics and Biostatistics, University of Medicine and Pharmacy of Craiova, Romania*

[10)]*Department of Anesthesiology and Intensive Care, University of Medicine and Pharmacy of Craiova, Romania*

[11)]*Department of Anatomy and Embryology, Victor Babeş University of Medicine and Pharmacy, Timişoara, Romania*

[12)]*PhD Student, Doctoral School, Victor Babeş University of Medicine and Pharmacy, Timişoara, Romania*

Abstract

Objectives: This study aims to establish a correlation between placental histopathological and immunohistochemical (IHC) changes and preterm birth with fetal growth restriction (FGR, formerly called intrauterine growth restriction – IUGR). *Patients, Materials, and Methods*: This prospective study was performed on a group of 30 parturients, with singleton gestation, of which 15 patients gave birth at term, and the other 15 patients gave birth prematurely. After the statistical correlation of the clinical and demographic data with premature birth (PB) and term birth (TB), we performed histological and IHC research on the respective placentae. To observe normal and pathological microscopic placental structures, we used the Hematoxylin–Eosin (HE) and Periodic Acid Schiff–Hematoxylin (PAS-H) classical stainings, but also special immunostaining with anti-cluster of differentiation 34 (CD34) and anti-vascular endothelial growth factor (VEGF) antibodies. *Results*: We found a statistically significant difference between the TB/PB categories and the age of the patients, their *antepartum* weight, the weight of the newborns, and the placenta according to the sex of the newborn. Histological analysis revealed in the case of TB, small areas of perivillous amyloid deposition, with the significant extension of these areas both intravillous and perivillous in the case of PB. Massive intravillous calcifications, syncytial knots, and intravillous vascular thrombosis were also frequently present in PB. With PAS-H staining were highlighted the intra/extravillous vascular basement membranes, but especially the massive fibrin deposits rich in glycosaminoglycans. By the IHC technique with the anti-CD34 antibody, we noticed the numerical vascular density, higher in the case of TB, but in the case of PB, there were large areas of placental infarction, with a lack of immunostaining in these areas. Through the anti-VEGF antibody, we observed the presence of signal proteins that determined and stimulated the formation of neoformation vessels in the areas affected by the lack of post-infarction placental vascularization. We observed a highly significant difference between placental vascular density between TB/PB and newborn weight, sex, or placental weight. *Conclusions*: Any direct proportional link between the clinical maternal–fetal and histological elements yet studied must be considered. Thus, establishing an *antepartum* risk group can prevent a poor pregnancy outcome.

Keywords: placenta, fibrin depositions, placental infarction, syncytial knot, vascular density, preterm birth.

Introduction

It has long been known that premature birth (PB) is a leading cause of perinatal morbidity and mortality [1] being responsible for 35% of neonatal deaths [2]. The etiology of PB is multifactorial [3], the precise cause of PB is difficult to quantify, two-thirds of PBs are idiopathic and one-third of iatrogenic causes, to maternal and fetal reasons [4, 5]. One cause, that is still underestimated for idiopathic PB, may be placental dysfunction in which placental changes appear to be closely related to oxidative stress [6]. As described, it appears that placental dysfunction is characterized by accelerated placental villous hypermaturation, which is associated with increased syncytial knotting, and the massive perivillous fibrin depositions, rich in glycosaminoglycans and mucopolysaccharides [7–9]. These placental changes are characteristic of severe preeclampsia (P) and late intrauterine growth restriction (IUGR) but have also been

This is an open-access article distributed under the terms of a Creative Commons Attribution-NonCommercial-ShareAlike 4.0 International Public License, which permits unrestricted use, adaptation, distribution and reproduction in any medium, non-commercially, provided the new creations are licensed under identical terms as the original work and the original work is properly cited.

observed in idiopathic PB [6]. Unlike late-onset IUGR, severe early-onset IUGR is characterized by distal villous hypomaturation [9, 10]. This abnormal development of the placental villous tree influences the placental exchanges due to the quantitative decrease of the terminal villi, as well as the deterioration of the syncytiotrophoblast, at the level of which the maternal–fetal exchange takes place [11, 12].

These disorders of villous anomalies, which are hallmarks of a placental lesion that is associated with hypoxia, can lead to fetal death [13]. On the other hand, regarding maternal health, women who had a PB may develop a cardiometabolic pathology in the decade after pregnancy and have an atherogenic lipid profile. Although the study of the placenta dates back decades, knowing that its proper functioning is the most important element for fetal and neonatal health, in recent years this hypothesis has been induced that future maternal health may have placental indications [14]. Therefore, in both maternal and fetal interest, the placenta from PB should be investigated histologically, for fetal and maternal well-being.

Aim

This study aims to establish a correlation between placental histological and immunohistochemical (IHC) changes and PB with fetal growth restriction (FGR), compared with placental changes in normal term pregnancy (TP). Microscopic structural and vascular placental changes present in singleton TP or prematurity have been associated with coexisting maternal and fetal clinical features.

Patients, Materials and Methods

This study was performed on a group of 30 parturients, with singleton gestation. Of these, 15 patients gave birth at term, after 37 weeks of pregnancy, and the other 15 patients gave birth prematurely, between 32–35.6 weeks of gestation. The patients included in the study were hospitalized and gave birth in the Department of Obstetrics and Gynecology, Emergency County Hospital, Craiova, and in the Department of Obstetrics and Gynecology, Filantropia Municipal Hospital, Craiova, Romania, between January 2020–January 2022. Exclusion criteria from the study referred to chronic maternal pathology, preterm prelabor rupture of the membranes, multiple gestations, fetal congenital anomalies, *placenta praevia*, and any other vaginal bleeding. At the first monitoring visit, an interview was conducted, which included the main demographic, clinical, and medical data.

Ethical consideration

Pregnant women participating in the study expressed written informed consent for the use of placental samples and maternal and fetal clinical data. Based on the Declaration of Helsinki, the Ethics Committee of the University of Medicine and Pharmacy of Craiova approved this study.

Histopathological and IHC study

Immediately after birth, the placentae were taken, weighed, washed, and photographed, and tissue fragments were collected from each. The placental tissue taken was sent to the Research Center for Microscopic Morphology and Immunology, University of Medicine and Pharmacy of Craiova, to be included in paraffin, sectioned using the microtome, stained by classical and IHC techniques, and analyzed.

Fixation of placental tissue was performed with 10% neutral buffered formalin, at room temperature, for 10 days. The paraffin inclusion took place according to the following protocol: the tissues were washed for a few hours in a continuous jet of tap water, dehydrated with alcohol at increasing concentrations, as follows: 70% (12 hours), 90%, 96%, 100% (1–2 hours/alcohol bath), then moved successively to three xylene baths (three hours in total). From xylene, the placental tissue fragments were introduced into molten paraffin (56°C for one day). After 24 hours, the solid paraffin blocks were obtained. The placentae thus processed were sectioned using the HM350 rotary microtome, equipped with a system to transfer water bath sections (STS microM) to a thickness of 5 μm, and the slices obtained were mounted on simple slides for classical histological studies, as well as on slides with poly-L-lysine for IHC studies. The tissue applied to the slides was left to dry in the thermostat for one day at 37°C. To observe normal and pathological microscopic placental structures, we used the Hematoxylin–Eosin (HE) and Periodic Acid Schiff–Hematoxylin (PAS-H) classical stainings, but also special IHC labeling with anti-cluster of differentiation 34 (CD34) antibody to mark the presence of capillary endothelium in intravillous neoformation of blood vessels and the anti-vascular endothelial growth factor (VEGF) antibody that label certain proteins that determine and stimulate the formation of blood vessels.

For both classical and special IHC studies, the slides were deparaffined in xylene glass containers (3×10 minutes), and the placental tissues were dehydrated with alcohol with decreasing concentrations (100%, 96%, 90%, and 70% – 5 minutes/each alcohol bath), then the tissues were rehydrated with distilled water (dH_2O) (3×5 minutes/bath). After this step, the protocol varied depending on the staining technique. Through the classical HE staining technique, we highlighted the nuclei with Hematoxylin and the collagen fibers with the Eosin solution. Placental glycosaminoglycans were highlighted by the PAS-H technique. The placental tissue applied on the slides with poly-L-lysine was delimited with a hydrophobic marker (DakoPen), then the antigenic unmasking in pH 6 citrate solution was done by boiling in the microwave oven (650 W, seven cycles × 3 minutes). After cooling, the slides were washed with dH_2O (3×5 minutes), and endogenous peroxidase inactivation was attempted by using 2% hydrogen peroxide (H_2O_2) for 30 minutes. H_2O_2 was subsequently removed from the tissues by abundant washing in dH_2O and the slides were introduced into the 1% phosphate-buffered saline (PBS) for five minutes. Before application of the primary antibody, non-specific sites were blocked using 3% skim milk solution (30 minutes), and only after this step was the primary antibody dripped (Table 1). The slides thus obtained were placed in the refrigerator for 18 hours at 4°C. The next day, the slides were brought to room temperature, washed in 1% PBS to remove the primary antibody, and the secondary antibody [mouse VC002-025, R&D Systems, VisUCyte Horseradish Peroxidase (HRP) Polymer] was applied over the tissue for 1–2 hours, during which time the secondary antibody binds to the primary antibody and helps amplify the subsequent, post-development reaction. The secondary

antibody was then removed with 1% PBS and 3,3'-Diaminobenzidine (DAB) (Dako) was used to develop slides. The nuclei were labeled with Hematoxylin. To complete the slides, the tissue was dehydrated in successive alcohol baths with increasing concentrations (70%, 90%, 96%, and 100% – 5 minutes/each alcohol bath), the slides were clarified in xylene containers for 45 minutes (3×15 minutes/bath) and 24×50 mm slides with Canadian conditioner were mounted.

Table 1 – *IHC panel of antibodies used by us*

Antibody	Manufacturer	Clone	Antigenic exposure	Secondary antibody	Dilution	Labeling
Anti-CD34	Dako	QBEnd/10	Citrate, pH 6	Monoclonal mouse anti-human CD34 Class II	1:50	Neoformed blood vessels
Anti-VEGF	Dako	VG1	Citrate, pH 6	Monoclonal mouse anti-human VEGF	1:50	A signal protein that stimulates the formation of blood vessels

CD34: Cluster of differentiation 34; IHC: Immunohistochemical; VEGF: Vascular endothelial growth factor.

To quantify the vascular density immunolabeled with the anti-CD34 antibody, we made four images with the ×200 objective from the same placental scanned slide of each case (15 cases – TB, 15 cases – PB). After photographing the sections, the small blood vessels in the structure of the placental villi were counted, but also the perivillous ones of each case, with the help of the ImageProPlus program, and we structured a statistical table with a comparative note in the Microsoft XL 2010 program.

Statistical analysis

With the help of the Microsoft Excel 2010 program, we elaborated various statistical and comparative studies through the *t*-test, analysis of variance (ANOVA) Single Factor test regarding the clinical data of the mothers (age, weight), the newborns (weight, sex), as well as on placental microscopic vascular aspects.

Results

Patients with a gestational age over 37 weeks were 19–46 years old, with a mean age of 29.73 years (±8.48 years), and patients who gave PB were 25–43 years old, with an average age of 34.73 years (±5.32 years). Applying the Two-Sample *t*-test Assuming Equal Variances, we noticed a statistically significant difference between the two TB/PB categories in terms of patient age, $t(15)=-1.933$, $p=0.03$ (Figure 1). The *antepartum* weight of the 30 pregnant women varied in the case of patients with TB between 65–101 kg, with an average of 79.86 kg (±10.02 kg), and in the case of patients with PB, it varied between 76–114 kg, with an average of 91.13 kg (±9.4 kg). Applying the Two-Sample *t*-test Assuming Equal Variances, we noticed a statistically significant difference between the two TB/PB categories in terms of patients' *antepartum* weight, $t(15)=-3.174$, $p=0.001$ (Figure 2).

Full-term or premature infants included in the study were grouped by sex, so in the case of TB, we had seven female newborns (TNB-F) and eight male newborns (TNB-M), and in the case of PB, we had nine female newborns (PNB-F) and six male newborns (PNB-M). Applying the χ^2 (*chi*-squared) test, we noticed that the distribution of newborns by sex was not significantly different (Figure 3).

The weight of TNB-F ranged from 2660–3500 g, with an average value of 3068.57 g (±266.86 g), and the weight of TNB-M varied between 2915–3990 g, with an average value of 3301.25 g (±467.7 g). The weight of PNB-F ranged between 1980–2540 g, with an average value of 2270.55 g (±179.45 g), and the weight of PNB-M varied between 2030–2800 g, with an average value of 2343.33 g (±272 g). By applying the ANOVA Single Factor test, we noticed a highly significant difference between the weights of the newborns for these groups, $F(3.29)=20.784$, $p<0.001$ (Figure 4). The TNB-F placenta weighed between 443–583 g, with an average value of 511.14 g (±44.50 g), at TNB-M it varied between 485–665 g, with an average value of 617.75 g (±97.41 g). In PNB-F, the weight ranged between 310–480 g, with an average value of 387.55 g (±56.33 g), and in PNB-M the weight varied between 320–480 g, with an average value of 416.33 g (±57.62 g). Applying the ANOVA Single Factor test, we observed that there was a highly significant overall difference between the placental weight for these groups, $F(3.29)=18.698$, $p<0.001$ (Figure 5).

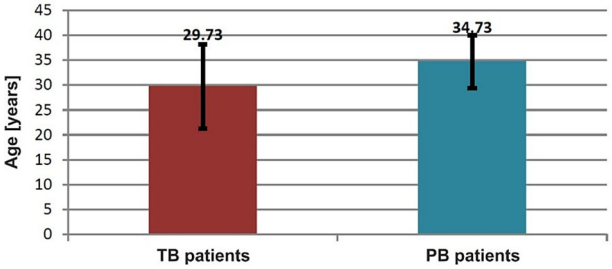

Figure 1 – *The average age (years) of the pregnant women included in the study. Pregnant women's average age was significantly lower for those with TB compared to those with PB, t(15)=-1.933, p=0.03. PB: Premature birth; TB: Term birth.*

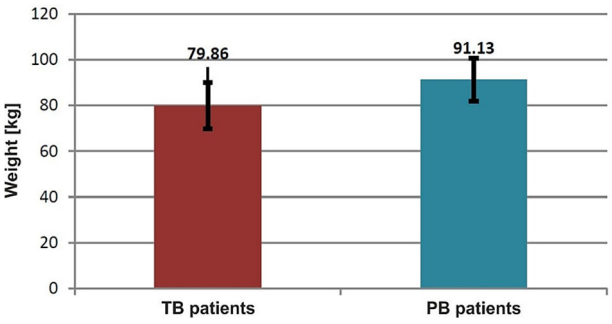

Figure 2 – *The average weight (kg) of the pregnant women included in the study. Pregnant women's average weight was significantly lower for the TB cases (79.86± 10.02 kg) compared to those with PB (91.13±9.4 kg), t(15)=-3.174, p=0.001. PB: Premature birth; TB: Term birth.*

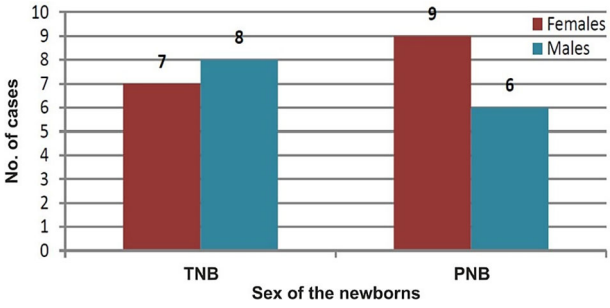

Figure 3 – ***The distribution of males/females newborn was not significantly different for the newborn group of TB/PB, $\chi^2(2, N=30)=1.534$, $p=0.46$. PB: Premature birth; PNB: Premature newborn; TB: Term birth; TNB: Term newborn.***

The placental macroscopic aspects of both the TB and PB groups highlighted the two placental surfaces (maternal and fetal side), the existence of amniotic membranes, the umbilical cord on the placental fetal side (Figures 6 and 7), and the placental microscopic morphology in these two groups revealed various structural changes characteristic of TB and PB (Figures 8 and 9).

Through the classical HE staining technique, we highlighted both the normal structure of placental villi, with collagen fibers stained in pink, the syncytiotrophoblast present at the periphery of the villi, but also some structural changes present: variable fibrinoid deposits (stained in pink), massive calcifications (stained in blue-violet), syncytial knots present at the villous periphery, intravascular thrombosis (stained in red), infarcts (weakly stained areas, without vascularization) (Figures 8 and 9).

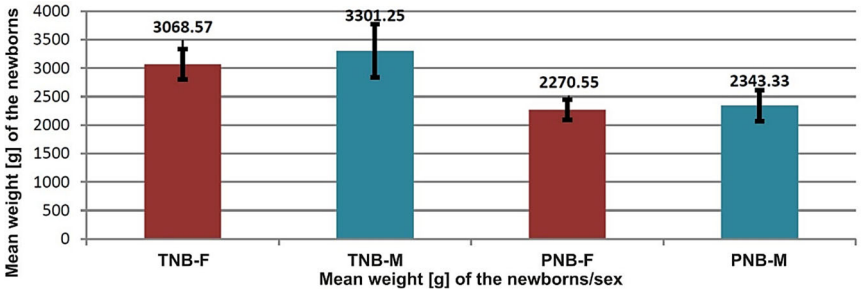

Figure 4 – ***Mean weight of fetuses according to the type of TB/PB and to the sex of the newborn. There was a highly significant difference between the weight of the newborns for these groups, $F(3,29)=20.784$, $p<0.001$. F: Female; M: Male; PB: Premature birth; PNB: Premature newborn; TB: Term birth; TNB: Term newborn.***

Figure 5 – ***Mean placental weight of fetuses, according to the type of TB/PB and to the sex of the newborn. There was a highly significant difference between the placental weight of the newborns for these groups, $F(3,29)=18.689$, $p<0.001$. F: Female; M: Male; PB: Premature birth; PNB: Premature newborn; TB: Term birth; TNB: Term newborn.***

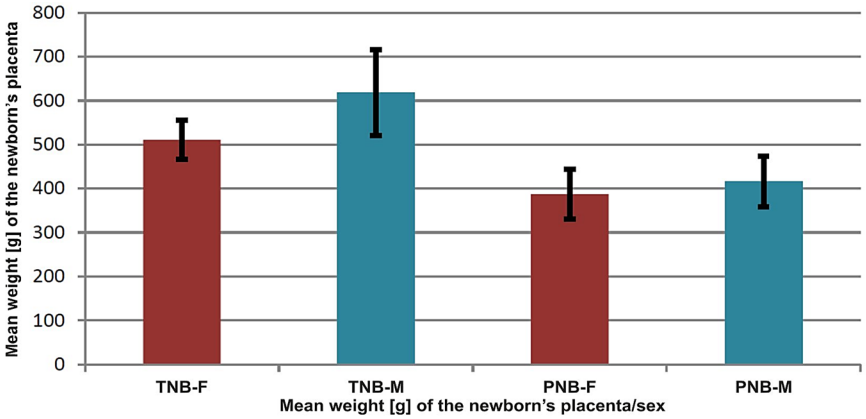

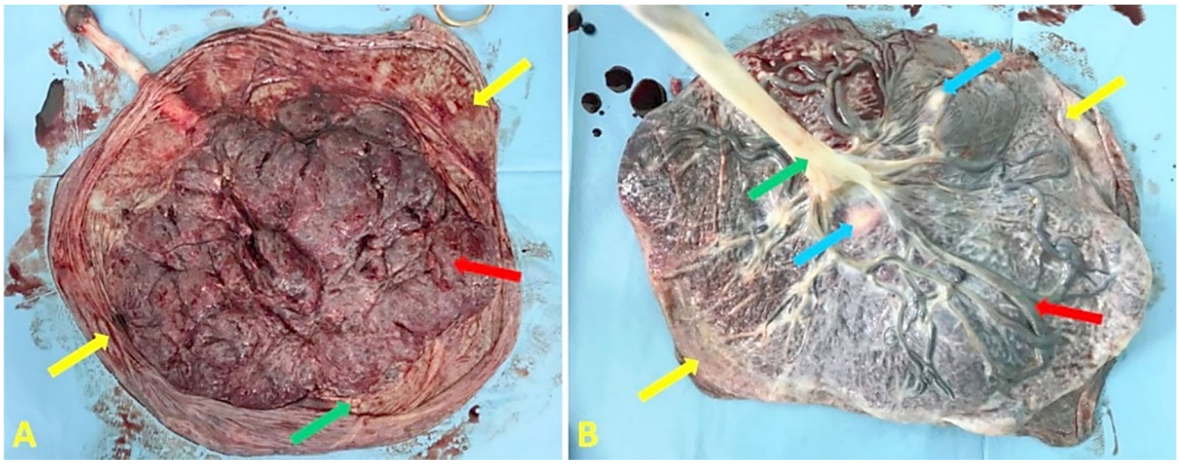

Figure 6 – ***Normal macroscopic morphological aspects of the placenta at term, from a singleton pregnancy, without pathological history associated with pregnancy – control group: (A) Placental maternal side – amniotic membranes (yellow arrows), small calcifications, and peripheral fibrin deposits, specific to the placenta at the end of the third trimester of pregnancy (green arrow) and normal placental cotyledons (red arrow) are observed; (B) Fetal placental side – the amniotic membranes covering the placenta (yellow arrows), the umbilical cord inserted in the central level (green arrow), the presence of fibrillar deposits (blue arrows) and the presence of normal placental vascularization (red arrow) are observed. Images from the collection of Dr. Anca-Maria Istrate-Ofițeru.***

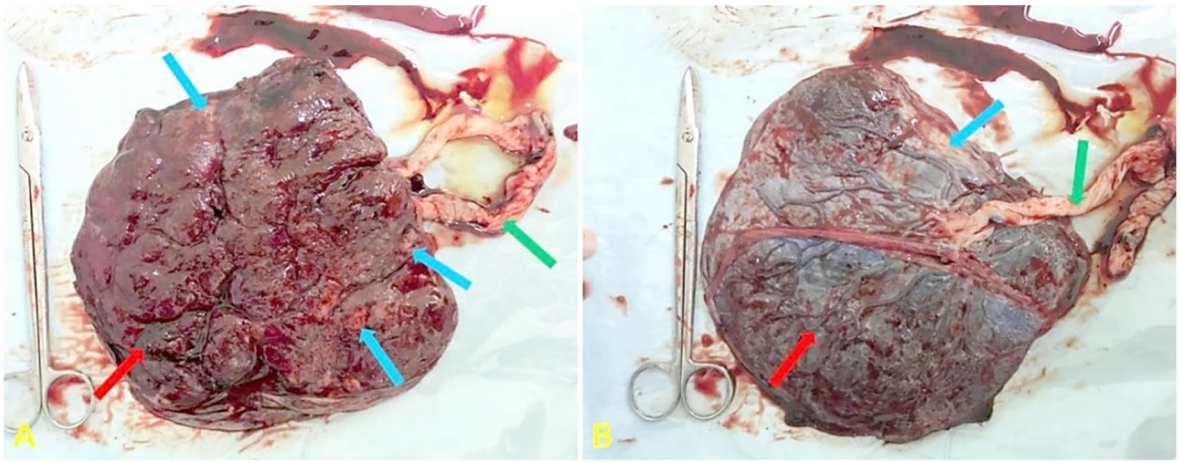

Figure 7 – ***Macroscopic morphopathological aspects of the placenta, a premature singleton pregnancy: (A) Placental maternal side – amniotic membranes are identified at the placental periphery, umbilical cord (green arrow), the presence of macroscopically visible thrombosis (red arrow), and placental cotyledons with large areas of fibrillar deposits and calcifications (blue arrows); (B) Fetal placental side – the amniotic membranes covering the placenta, the umbilical cord inserted paracentral (green arrow), the large fibrin deposits and placental calcifications (blue arrow) and the smaller caliber vascularization (red arrow) is observed. Images from the collection of Dr. Anca-Maria Istrate-Ofițeru.***

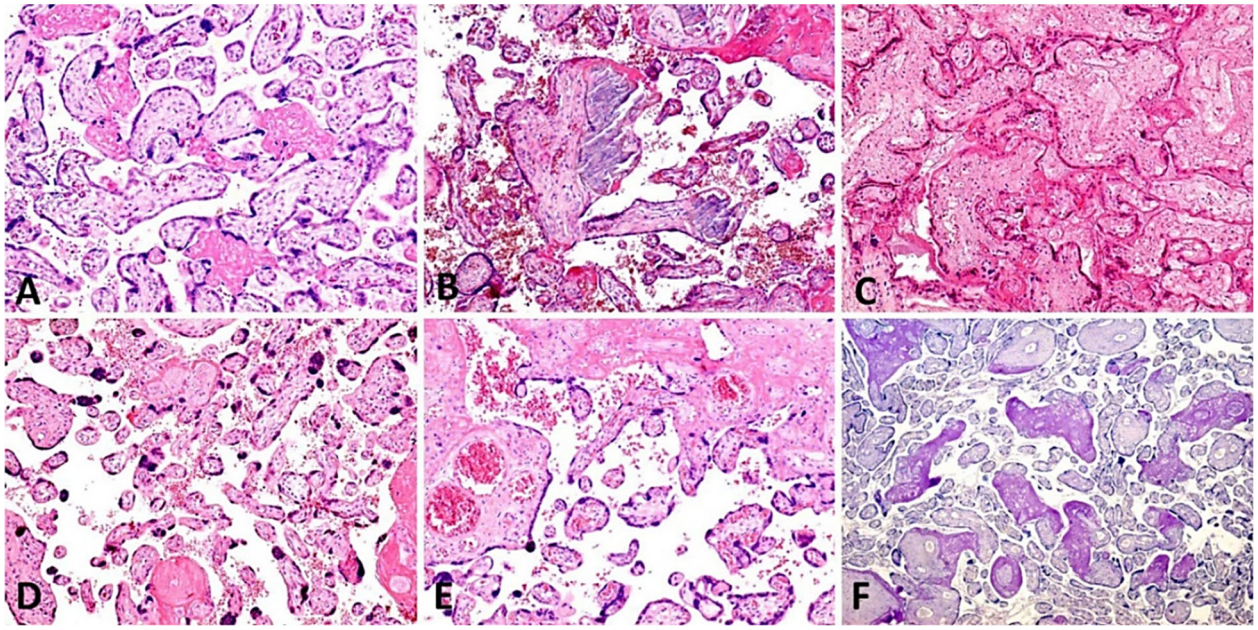

Figure 8 – ***Morphological and morphopathological microscopic aspects of the TB and PB placenta: (A) Placental villi with normal appearance and perivillous fibrinoid deposition areas specific to TB; (B) Placental villi from PB with large areas of calcification (blue-purple areas) and perivillous fibrinoid deposits (pink areas); (C) Placental villi from PB with normally modified aspect, with large areas of perivillous and intravillous fibrinoid deposition (stained in pink); (D) Placental villi from PB, with areas of placental infarction (bottom of the image) and the presence of multiple syncytial knots (blue areas); (E) PB placental villi with large areas of amyloid deposition and multiple thrombosed intravillous blood vessels (red areas); (F) PB placental villi with large areas of perivillous and intravillous amyloid deposition. HE staining: (A–E) ×200. PAS-H staining: (F) ×200. HE: Hematoxylin–Eosin; PAS-H: Periodic Acid Schiff–Hematoxylin; PB: Premature birth; TB: Term birth. Images from the collection of Dr. Anca-Maria Istrate-Ofițeru.***

In the case of TB, small areas of perivillous amyloid deposition may be present (Figure 8A), but in the case of PB, these areas are much larger both intravillous and perivillous (Figure 8, B–E). Also, in the case of PB, we frequently noticed the presence of massive intravillous calcifications (Figure 8B), syncytial knots (Figure 8D), as well as intravillous vascular thrombosis (Figure 8E). Using PAS-H staining, we highlighted intra/extravillous vascular basement membranes, but especially the massive fibrin deposits rich in glycosaminoglycans (intense pink areas) (Figure 8F).

Through the special IHC technique, we immunolabeled using anti-CD34 antibody the intravillous capillary endothelial cells (stained in brown) – small vessels of neoformation, which helped to obtain the numerical vascular density, which was higher in the control group – TB. Also, through this immunostaining, we noticed that in TB the vascularization had a normal intravillous distribution, but in the case of PB, there were large areas of placental infarction, with a lack of immunostaining in these areas (Figure 9, A and B). Using anti-VEGF antibody, we observed the presence of signal proteins that favored and stimulated the formation of neoformation vessels in the areas affected by the lack of vascularization, at the level of placental infarction (Figure 9, C and D).

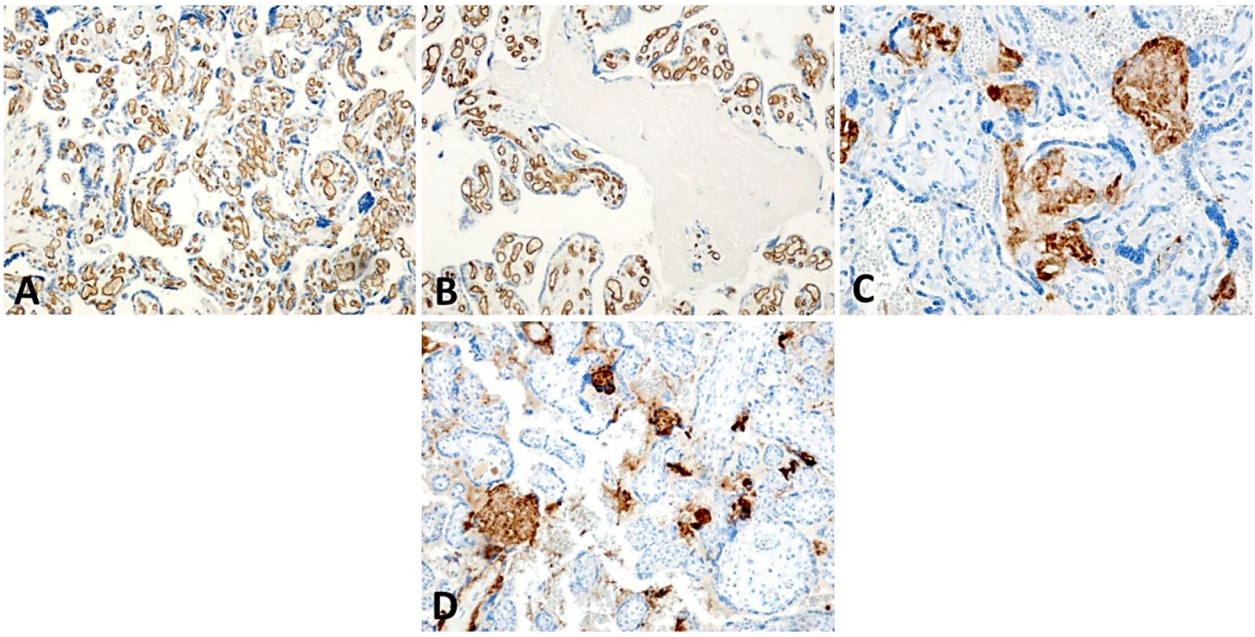

Figure 9 – ***IHC microscopic morphological and morphopathological aspects of the TB and PB placenta: (A) Placental villi with a normal appearance from TB, with placental villi presenting intravillous capillaries with normal numerical density, immunolabeled at endothelial level using anti-CD34 antibody; (B) Infarcted placental villi from PB, with the absence of endothelial immunolabeling at this level and its presence in the capillaries that have not yet undergone infarction processes; (C and D) Normal and pathological placental villi, with intravillous infarction areas in PB; the presence of VEGF immunoreactivity in the affected areas was observed. IHC staining with anti-CD34 antibody: (A) ×100; (B) ×200. IHC staining with anti-VEGF antibody: (C) ×100; (D) ×200. CD34: Cluster of differentiation 34; IHC: Immunohistochemical; PB: Premature birth; TB: Term birth; VEGF: Vascular endothelial growth factor. Images from the collection of Dr. Anca-Maria Istrate-Ofițeru.***

We obtained statistical values that reveal that the number of blood vessels is higher in the placental structure in TB, compared to the number of vessels in PB. The vascular density of the placenta associated with TNB-F had values between 125.5–150.75 vessels/×200, with an average value of 137.32 vessels/×200 (±8.34 vessels/×200), and in the case of TNB-M, the vascular density ranged from 125.5–150.75 vessels/×200, with an average value of 138.46 vessels/×200 (±8.37 vessels/×200).

In the case of PNB-F, the vascular density varied between 100.25–125 vessels/×200, with an average value of 113.27 vessels/×200 (±8.94 vessels/×200), and in the case of PNB-M, the vascular density varied between 100.25–123.25 vessels/×200, with an average value of 114.83 vessels/×200 (±9.36 vessels/×200). Applying the ANOVA Single Factor test, we observed that there was a highly significant difference between placental vascular densities in these groups, $F(3.29)=18.945$, $p<0.001$ (Figure 10).

We also performed several comparative studies on the weight of patients and age and noticed that they can increase in a directly proportional relationship, and by applying the Two-Sample *t*-test Assuming Equal Variances between categories, we noticed that there are statistically significant differences between mother's weight, age, and newborn's sex (Figure 11; Table 2). A directly proportional increase was also present in the comparative study in terms of fetal weight and placental weight. And in this case, by applying the Two-Sample *t*-test Assuming Equal Variances between categories, we observed that there are statistically significant differences between the weight of the fetus by sex and the weight of its placenta (Figure 12; Table 3).

Regarding the comparative study between fetal weight and vascular density, we observed that there is a proportional increase between these categories, and by applying Two-Sample *t*-test Assuming Equal Variances between categories, we noticed that there are statistically significant differences between weight and sex of the newborn and vascular density (Figure 13; Table 4).

Table 2 – ***Comparison between age, the weight of the patients, and sex of the newborn, according to the type of TB/PB***

	TNB-F patients	TNB-M patients	PNB-F patients	PNB-M patients
t Stat	-9.794	-10.672	-14.571	-14.937
P(*T*<=*t*) one-tail	<0.001	<0.001	<0.001	<0.001

F: Female; M: Male; PB: Premature birth; PNB: Premature newborn; TB: Term birth; TNB: Term newborn.

Table 3 – ***Comparison between the mean fetal weight and the mean placental weight of the newborns, according to the type of TB/PB***

	TNB-F patients	TNB-M patients	PNB-F patients	PNB-M patients
t Stat	25.009	15.887	30.034	16.976
P(*T*<=*t*) one-tail	<0.001	<0.001	<0.001	<0.001

F: Female; M: Male; PB: Premature birth; PNB: Premature newborn; TB: Term birth; TNB: Term newborn.

Table 4 – ***Comparison between mean fetal weight and placental vascular density, according to the type of TB/PB***

	TNB-F patients	TNB-M patients	PNB-F patients	PNB-M patients
t Stat	29.047	19.123	36.019	20.056
P(*T*<=*t*) one-tail	<0.001	<0.001	<0.001	<0.001

F: Female; M: Male; PB: Premature birth; PNB: Premature newborn; TB: Term birth; TNB: Term newborn.

At the end of these clinical-statistical comparisons, we noticed that the placental weight varies in direct proportion to the placental vascular density, and by applying the Two-Sample *t*-test Assuming Equal Variances between categories, we noticed that there are statistically significant differences between the placental weight of newborn's sex and vascular density (Figure 14; Table 5).

Table 5 – ***Comparison between mean placental weight and placental vascular density, according to the type of TB/PB***

	TNB-F patients	TNB-M patients	PNB-F patients	PNB-M patients
t Stat	21.841	13.864	14.425	12.649
P(*T*<=*t*) one-tail	<0.001	<0.001	<0.001	<0.001

F: Female; M: Male; PB: Premature birth; PNB: Premature newborn; TB: Term birth; TNB: Term newborn.

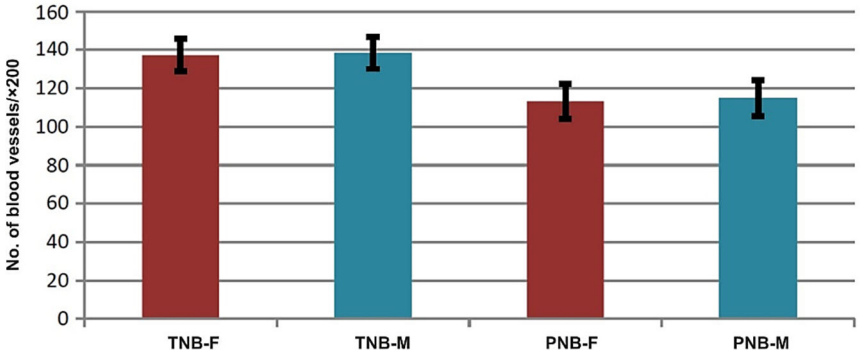

Figure 10 – ***Mean vascular density from the placenta of the patients with TB/PB. There was a highly significant difference between the number of blood vessels/×200 of the newborn's placenta for these groups, F(3,29)=18.945, p<0.001. F: Female; M: Male; PB: Premature birth; PNB: Premature newborn; TB: Term birth; TNB: Term newborn.***

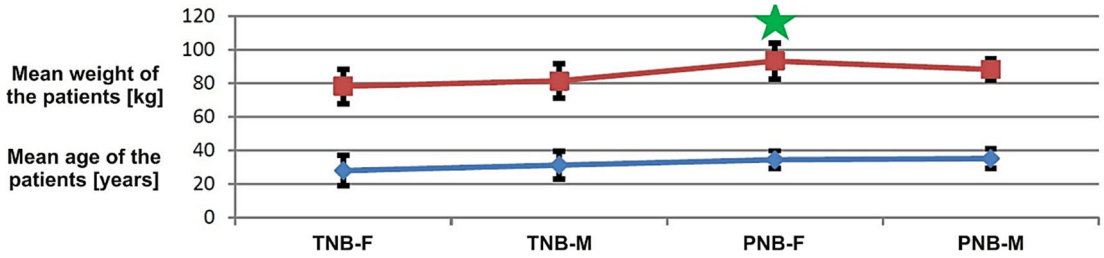

Figure 11 – ***Comparison between the mean age of the patients according to the type of TB/PB, sex of the newborn, and maternal weight. It was observed that there was a directly proportional relationship between their values (green asterisk). F: Female; M: Male; PB: Premature birth; PNB: Premature newborn; TB: Term birth; TNB: Term newborn.***

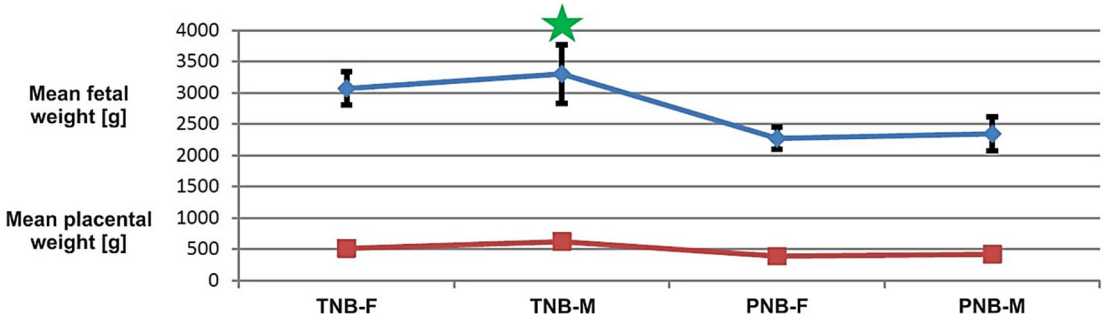

Figure 12 – ***Comparison between the mean fetal weight and the mean placental weight according to the type of TB/PB and sex of the newborn. We observed that fetal weight values increase in direct proportion to placental weight values (green asterisk). F: Female; M: Male; PB: Premature birth; PNB: Premature newborn; TB: Term birth; TNB: Term newborn.***

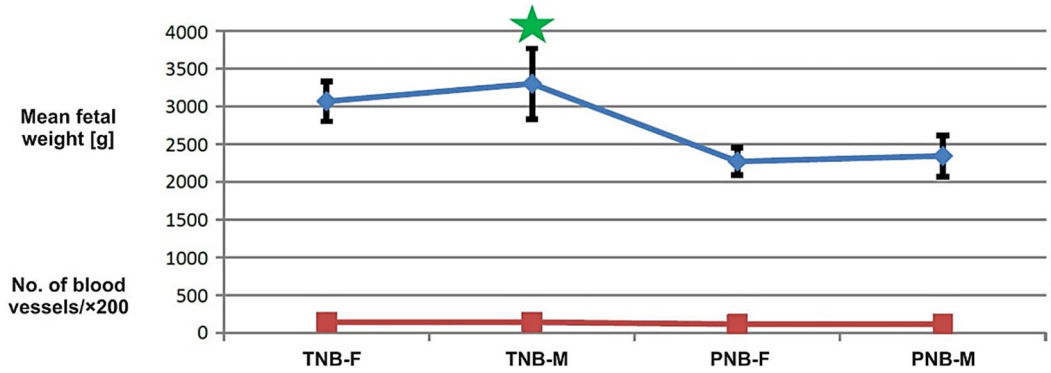

Figure 13 – ***Comparison between mean fetal weight and placental vascular density. We noticed that the fetal weight values increase directly to the placental vascular density (green asterisk). F: Female; M: Male; PNB: Premature newborn; TNB: Term newborn.***

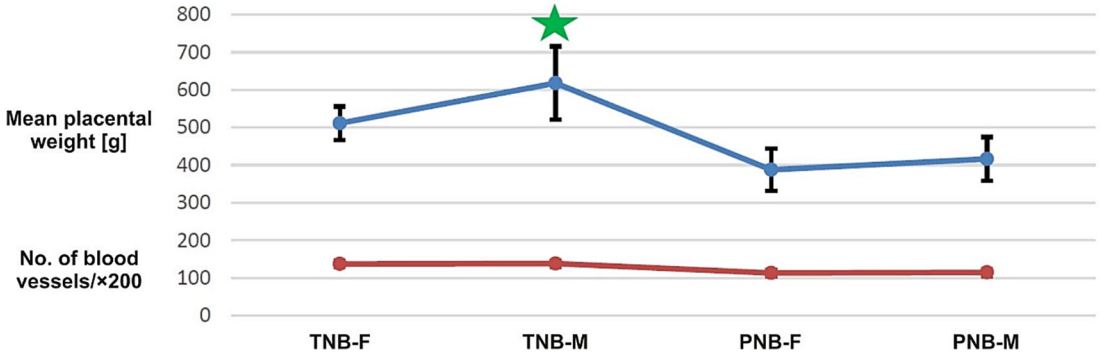

Figure 14 – ***Comparison between mean placental weight and placental vascular density. We noticed that the mean placental weight values increase directly to the placental vascular density (green asterisk). F: Female; M: Male; PNB: Premature newborn; TNB: Term newborn.***

Discussions

A good placental function is the key to good fetal development. In contrast, impaired placental function can lead to an increased risk for the fetus to develop an IUGR and even PB. Over time, researchers have tried to understand how these pregnancy complications can be explained in terms of placental changes [15–20]. The morphopathological analysis of the placenta is frequently used in the literature to detect the possible cause of both PB and IUGR. An important mechanism by which the placenta can cause these pathologies is represented by abnormalities of the fetoplacental circulation, which cause an increase in placental vascular resistance [21, 22].

In our study, in addition to the placental microscopic evaluation, we tried to see if the clinical parameters are also involved in the production of PB. Globally, in recent decades, with the increase in the PB rate, there is an increase in maternal age, but this relationship remains controversial. While some studies have found that maternal age is independently associated with PB [23, 24], other studies have noted that both advanced maternal age and younger age have the same risk of PB [25]. The results of our study showed a mean age of 34.73 years (±5.32 years) in patients with PB, compared to 29.73 years (±8.48 years) in patients with TB, noting that there was a statistically significant difference between the two categories of TB/PB in terms of patient age. We also found a statistically significant difference between *antepartum* maternal weight and PB. Although this issue is still controversial in the literature, some studies have shown that especially excessive gestational weight gain and underweight were associated with a higher probability of PB [26, 27].

There is a known increased risk of male sex mortality during pregnancy and neonatal period, with a higher percentage of male newborns in PB [28, 29]. But in our study, we observed that the distribution of newborns by sex was not significantly different, but we noted that there was a highly significant overall difference between the weight of newborns for these groups, females and males, and between placental weight and sex of newborns ($p<0.001$).

Placental pathology is an important contribution to PB, with lesions of a maternal vascular malfunction being the most common in PB [30, 31]. At present, in developed countries, for the evaluation of pregnancy complications, the study of the placenta has become a common thing. The *American College of Pathologists* published, in 1997, the guidelines for the study of placentae in high-risk pregnancies [32]. Later, a series of studies led by Redline [33] about a several criteria for diagnosing placental lesions and clinical correlation [33]. These criteria and definitions of placental lesions were updated in 2016 [34]. Evaluation of placental histopathological lesions in normal pregnancies shows that approximately 78% of cases presented placentae with various histological lesions, and 40% of cases had multiple lesions [35].

Our study, using the classical HE staining technique, showed both the normal structure of placental villi, with collagen fibers stained in pink, the presence of syncytiotrophoblast at the periphery of villi, but also some structural changes: variable fibrinoid deposits, massive calcifications, syncytial knots present in the peripheral villous area, intravascular thrombosis, placental infarction. In the case of TB, we noticed small areas of perivillous amyloid deposition, but in the case of PB, these areas were much larger both intravillous and perivillous. The histopathological findings frequently found in PB associated with IUGR were the presence of massive intravillous calcifications, syncytial knots, and intravillous vascular thrombosis. But we believe that the presence of syncytial knots, intravillous microcalcifications, and placental infarction over 5%, may cause the development of a IUGR and likely trigger PB. With these results, we are consistent with other studies [36, 37]. With the help of PAS-H staining, we highlighted the intra/extravillous vascular basement membranes, but especially the massive fibrin deposits present, rich in glycosaminoglycans. The frequency of histological lesions was higher in placentae from PB than in placentae from a full-TB. These findings are consistent with other studies in the literature [38].

By IHC technique, we immunolabeled using anti-CD34 antibody the intravillous capillary endothelial cells, and small vessels of neoformation, which helped to obtain the numerical vascular density, which was higher in the case of the control group – TB. Also, through this immunostaining, we noticed that in TB the vascularization had a normal intravillous distribution, but in the case of PB, there were large areas of placental infarction, with a lack of immuno-

staining in these areas. Using anti-VEGF antibody, we observed the presence of signal proteins that favored and stimulated the formation of neoformation vessels in the areas affected by the lack of vascularization at the level of placental infarction. In a normal placenta, vasculogenesis, which means the *de novo* formation of new vessels, begins about 15 days after conception, followed by angiogenesis on the 21st day after conception, which means the multiplication of blood vessels in existing vessels. Through these phenomena, in the third trimester, capillary loops are developed and formed at the level of terminal villi, which increase the maternal–fetal exchange surface [39]. It was found that in placentae from FGR and PB, this capillary branching is less dense than in normal placenta [40].

These findings are consistent with the results of our study, with statistical values revealing that the number of blood vessels in the placental structure in TB is higher compared to the number of vessels in PB. In the case of the placental structure associated with full-TB, but differentiated by the sex of the newborn, we found a slightly higher vascular density in males, with an average value of 138.46 vessels/×200 (±8.37 vessels/×200). In the case of placental structure associated with PB with IUGR, vascular density was slightly higher, 114.83 vessels/×200 (±9.36 vessels/×200), in males, but much lower than with normal pregnancy. We also noticed a highly significant difference between the weight and sex of the newborn and the vascular density, $p<0.001$. We noticed that the placental weight also varies directly proportional to the placental vascular density, there are statistically significant differences between the placental weight depending on the sex of the newborn and the vascular density, $p<0.001$. We noticed that the mean placental weight values increase directly proportional to the placental vascular density. Our findings are consistent with the studies of Tun *et al.* [41] and Berceanu *et al.* [42], which shows that these abnormalities in the placental vessels can influence the circulation of blood flow in the placental vascular system [41, 42].

Previous studies established that CD34 correlates with tumoral architecture [43–45], and with the current results, we established that it has different distribution also in non-tumor pathology. This, in turn, highlights the importance of vascularization in evolving tissues.

The histological and immunohistochemical images lack a standard in staining and using this could increase the impact of our results, as it has been previously shown [46] that a stain normalization technique would increase the morphometric accuracy of the tissues.

Starting from current results, we could use machine learning to obtain new predictive models that would push the knowledge further into clinical diagnosis systems. In similar approaches, morphometric observation on the revascularization in prostate adenocarcinoma [44, 45, 47] ended creating high-accuracy diagnosis tools [48, 49].

Conclusions

Probably these placental lesions that can occur throughout pregnancy and that act and stimulate each other, lead to those placental functional abnormalities, especially by the frequency and a greater amount of placental lesions, which cause a poor pregnancy outcome. Unfortunately, all these consequences of the presence of histological lesions are almost impossible to investigate *in vivo*. Therefore, any directly proportional link between the maternal–fetal clinical elements and the histological elements studied so far must be considered. Thus, establishing an *antepartum* risk group can prevent an unfavorable outcome of the pregnancy.

Conflict of interests

The authors declare that they have no conflict of interests.

Acknowledgments

Microscopic images have been acquired in the Research Center for Microscopic Morphology and Immunology, University of Medicine and Pharmacy of Craiova, Romania (Manager: Laurenţiu Mogoantă, Professor, MD, PhD).

Authors' contribution

Ioana Victoria Camen and Maria Magdalena Manolea equally contributed to this article.

References

[1] Kramer MS, Demissie K, Yang H, Platt RW, Sauvé R, Liston R. The contribution of mild and moderate preterm birth to infant mortality. Fetal and Infant Health Study Group of the Canadian Perinatal Surveillance System. JAMA, 2000, 284(7):843–849. https://doi.org/10.1001/jama.284.7.843 PMID: 10938173

[2] Chawanpaiboon S, Vogel JP, Moller AB, Lumbiganon P, Petzold M, Hogan D, Landoulsi S, Jampathong N, Kongwattanakul K, Laopaiboon M, Lewis C, Rattanakanokchai S, Teng DN, Thinkhamrop J, Watananirun K, Zhang J, Zhou W, Gülmezoglu AM. Global, regional, and national estimates of levels of preterm birth in 2014: a systematic review and modelling analysis. Lancet Glob Health, 2019, 7(1):e37–e46. https://doi.org/10.1016/S2214-109X(18)30451-0 PMID: 30389451 PMCID: PMC6293055

[3] Pereira L, Reddy AP, Alexander AL, Lu X, Lapidus JA, Gravett MG, Nagalla SR. Insights into the multifactorial nature of preterm birth: proteomic profiling of the maternal serum glycoproteome and maternal serum peptidome among women in preterm labor. Am J Obstet Gynecol, 2010, 202(6):555.e1–555.e10. https://doi.org/10.1016/j.ajog.2010.02.048 PMID: 20413102

[4] Goldenberg RL, Culhane JF, Iams JD, Romero R. Epidemiology and causes of preterm birth. Lancet, 2008, 371(9606):75–84. https://doi.org/10.1016/S0140-6736(08)60074-4 PMID: 18177778 PMCID: PMC7134569

[5] Romero R, Dey SK, Fisher SJ. Preterm labor: one syndrome, many causes. Science, 2014, 345(6198):760–765. https://doi.org/10.1126/science.1251816 PMID: 25124429 PMCID: PMC4191866

[6] Morgan TK, Tolosa JE, Mele L, Wapner RJ, Spong CY, Sorokin Y, Dudley DJ, Peaceman AM, Mercer BM, Thorp JM, O'Sullivan MJ, Ramin SM, Rouse DJ, Sibai B; Eunice Kennedy Shriver National Institute of Child Health and Human Development Maternal–Fetal Medicine Units Network. Placental villous hypermaturation is associated with idiopathic preterm birth. J Matern Fetal Neonatal Med, 2013, 26(7):647–653. https://doi.org/10.3109/14767058.2012.746297 PMID: 23130816 PMCID: PMC4010251

[7] Salafia CM, Vogel CA, Vintzileos AM, Bantham KF, Pezzullo J, Silberman L. Placental pathologic findings in preterm birth. Am J Obstet Gynecol, 1991, 165(4 Pt 1):934–938. https://doi.org/10.1016/0002-9378(91)90443-u PMID: 1951558

[8] Redline RW, Boyd T, Campbell V, Hyde S, Kaplan C, Khong TY, Prashner HR, Waters BL; Society for Pediatric Pathology, Perinatal Section, Maternal Vascular Perfusion Nosology Committee. Maternal vascular underperfusion: nosology and reproducibility of placental reaction patterns. Pediatr Dev Pathol, 2004, 7(3):237–249. https://doi.org/10.1007/s10024-003-8083-2 PMID: 15022063

[9] Kingdom J, Huppertz B, Seaward G, Kaufmann P. Development of the placental villous tree and its consequences for fetal growth. Eur J Obstet Gynecol Reprod Biol, 2000, 92(1):35–43. https://doi.org/10.1016/s0301-2115(00)00423-1 PMID: 10986432

[10] Istrate-Ofiţeru AM, Berceanu C, Berceanu S, Busuioc CJ, Roşu GC, Diţescu D, Grosu F, Voicu NL. The influence of gestational diabetes mellitus (GDM) and gestational hypertension (GH) on placental morphological changes. Rom J Morphol Embryol, 2020, 61(2):371–384. http://doi.org/10.47162/RJME.61.2.07 PMID: 33544789 PMCID: PMC7864320

[11] Burton GJ, Charnock-Jones DS, Jauniaux E. Regulation of vascular growth and function in the human placenta. Reproduction, 2009, 138(6):895–902. https://doi.org/10.1530/REP-09-0092 PMID: 19470597

[12] Vyberg M, Nielsen S. Proficiency testing in immunohistochemistry – experiences from Nordic Immunohistochemical Quality Control (NordiQC). Virchows Arch, 2016, 468(1):19–29. http://doi.org/10.1007/s00428-015-1829-1 PMID: 26306713 PMCID: PMC4751198

[13] Gluckman PD, Hanson MA, Cooper C, Thornburg KL. Effect of *in utero* and early-life conditions on adult health and disease. N Engl J Med, 2008, 359(1):61–73. https://doi.org/10.1056/NEJMra0708473 PMID: 18596274 PMCID: PMC3923653

[14] Parks WT, Catov JM. The placenta as a window to maternal vascular health. Obstet Gynecol Clin North Am, 2020, 47(1):17–28. https://doi.org/10.1016/j.ogc.2019.10.001 PMID: 32008667

[15] Kingdom JC, Audette MC, Hobson SR, Windrim RC, Morgen E. A placenta clinic approach to the diagnosis and management of fetal growth restriction. Am J Obstet Gynecol, 2018, 218(2S): S803–S817. https://doi.org/10.1016/j.ajog.2017.11.575 PMID: 29254754

[16] Kim YM, Chaemsaithong P, Romero R, Shaman M, Kim CJ, Kim JS, Qureshi F, Jacques SM, Ahmed AI, Chaiworapongsa T, Hassan SS, Yeo L, Korzeniewski SJ. Placental lesions associated with acute atherosis. J Matern Fetal Neonatal Med, 2015, 28(13):1554–1562. https://doi.org/10.3109/14767058.2014.960835 PMID: 25183023 PMCID: PMC4416076

[17] Jaiman S, Romero R, Pacora P, Erez O, Jung E, Tarca AL, Bhatti G, Yeo L, Kim YM, Kim CJ, Kim JS, Qureshi F, Jacques SM, Gomez-Lopez N, Hsu CD. Disorders of placental villous maturation are present in one-third of cases with spontaneous preterm labor. J Perinat Med, 2021, 49(4):412–430. https://doi.org/10.1515/jpm-2020-0138 PMID: 33554577 PMCID: PMC8324068

[18] Voicu NL, Bohîlţea RE, Berceanu S, Busuioc CJ, Roşu GC, Paitici Ş, Istrate-Ofiţeru AM, Berceanu C, Diţescu D. Evaluation of placental vascularization in thrombophilia and intrauterine growth restriction (IUGR). Rom J Morphol Embryol, 2020, 61(2): 465–476. https://doi.org/10.47162/RJME.61.2.16 PMID: 33544798 PMCID: PMC7864309

[19] Berceanu C, Tetileanu AV, Ofiţeru AM, Brătilă E, Mehedinţu C, Voicu NL, Szasz FA, Berceanu S, Vlădăreanu S, Navolan DB. Morphological and ultrasound findings in the placenta of diabetic pregnancy. Rom J Morphol Embryol, 2018, 59(1):175–186. PMID: 29940626

[20] Berceanu C, Ciurea EL, Cirstoiu MM, Berceanu S, Ofiteru AM, Mehedintu C, Berbece SI, Ciortea R, Stepan AE, Balseanu TA. Maternal–fetal management in thrombophilia related and placenta-mediated pregnancy complications. Rev Chim (Bucharest), 2018, 69(9):2396–2401. https://doi.org/10.37358/RC.18.9.6541 https://revistadechimie.ro/Articles.asp?ID=6541

[21] Pătru CL, Marinaş MC, Tudorache Ş, Căpitănescu RG, Sîrbu OC, Zorilă GL, Cernea N, Istrate-Ofiţeru AM, Roşu GC, Iovan L, Iliescu DG. The performance of hyperadherence markers in anterior *placenta praevia* overlying the Caesarean scar. Rom J Morphol Embryol, 2019, 60(3):861–867. PMID: 31912097

[22] Castellucci M, Kosanke G, Verdenelli F, Huppertz B, Kaufmann P. Villous sprouting: fundamental mechanisms of human placental development. Hum Reprod Update, 2000, 6(5):485–494. https://doi.org/10.1093/humupd/6.5.485 PMID: 11045879

[23] Fuchs F, Monet B, Ducruet T, Chaillet N, Audibert F. Effect of maternal age on the risk of preterm birth: a large cohort study. PLoS One, 2018, 13(1):e0191002. https://doi.org/10.1371/journal.pone.0191002 PMID: 29385154 PMCID: PMC5791955

[24] Voicu NL, Berceanu S, Paitici Ş, Roşu GC, Iovan L, Berceanu C, Bohîlţea RE, Istrate-Ofiţeru AM. Clinical and morphological study of single and twin pregnancies placenta. Curr Health Sci J, 2020, 46(1):44–55. https://doi.org/10.12865/CHSJ.46.01.07 PMID: 32637165 PMCID: PMC7323729

[25] Esposito G, Mauri PA, Cipriani S, Franchi M, Corrao G, Parazzini F. The role of maternal age on the risk of preterm birth among singletons and multiples: a retrospective cohort study in Lombardy, Norther Italy. BMC Pregnancy Childbirth, 2022, 22(1):234. https://doi.org/10.1186/s12884-022-04552-y PMID: 35317757 PMCID: PMC8941739

[26] Carnero AM, Mejía CR, García PJ. Rate of gestational weight gain, pre-pregnancy body mass index and preterm birth subtypes: a retrospective cohort study from Peru. BJOG, 2012, 119(8): 924–935. https://doi.org/10.1111/j.1471-0528.2012.03345.x PMID: 22607522 PMCID: PMC4112735

[27] Pigatti Silva F, Souza RT, Cecatti JG, Passini R Jr, Tedesco RP, Lajos GJ, Nomura ML, Rehder PM, Dias TZ, Oliveira PF, Silva CM; Brazilian Multicenter Study on Preterm Birth (EMIP) Study Group. Role of body mass index and gestational weight gain on preterm birth and adverse perinatal outcomes. Sci Rep, 2019, 9(1):13093. https://doi.org/10.1038/s41598-019-49704-x PMID: 31511664 PMCID: PMC6739338

[28] Stevenson DK, Verter J, Fanaroff AA, Oh W, Ehrenkranz RA, Shankaran S, Donovan EF, Wright LL, Lemons JA, Tyson JE, Korones SB, Bauer CR, Stoll BJ, Papile LA. Sex differences in outcomes of very low birthweight infants: the newborn male disadvantage. Arch Dis Child Fetal Neonatal Ed, 2000, 83(3): F182–F185. https://doi.org/10.1136/fn.83.3.f182 PMID: 11040165 PMCID: PMC1721180

[29] Peelen MJCS, Kazemier BM, Ravelli ACJ, De Groot CJM, Van Der Post JAM, Mol BWJ, Hajenius PJ, Kok M. Impact of fetal gender on the risk of preterm birth, a national cohort study. Acta Obstet Gynecol Scand, 2016, 95(9):1034–1041. https://doi.org/10.1111/aogs.12929 PMID: 27216473

[30] Nijman TAJ, van Vliet EOG, Benders MJN, Mol BWJ, Franx A, Nikkels PGJ, Oudijk MA. Placental histology in spontaneous and indicated preterm birth: a case control study. Placenta, 2016, 48:56–62. https://doi.org/10.1016/j.placenta.2016.10.006 PMID: 27871473

[31] Tetileanu AV, Berceanu C, Brătilă E, Navolan D, Ciortea R, Berceanu S, Cîrstoiu MM, Ofiţeru AM, Bohîlţea RE, Stepan AE, Mehedinţu C. Morphologic and ultrasound survey in type 2 diabetic placenta. Gineco.eu, 2018, 14(1):5–11. http://doi.org/10.18643/gieu.2018.5 http://gineco.eu/index.php/open/Morphologic%20and%20ultrasound%20survey%20in%20type%202%20diabetic%20placenta::74363

[32] Langston C, Kaplan C, Macpherson T, Manci E, Peevy K, Clark B, Murtagh C, Cox S, Glenn G. Practice guideline for examination of the placenta: developed by the Placental Pathology Practice Guideline Development Task Force of the College of American Pathologists. Arch Pathol Lab Med, 1997, 121(5):449–476. PMID: 9167599

[33] Redline RW. Placental pathology: a systematic approach with clinical correlations. Placenta, 2008, 29(Suppl A):S86–S91. https://doi.org/10.1016/j.placenta.2007.09.003 PMID: 17950457

[34] Khong TY, Mooney EE, Ariel I, Balmus NCM, Boyd TK, Brundler MA, Derricott H, Evans MJ, Faye-Petersen OM, Gillan JE, Heazell AEP, Heller DS, Jacques SM, Keating S, Kelehan P, Maes A, McKay EM, Morgan TK, Nikkels PGJ, Parks WT, Redline RW, Scheimberg I, Schoots MH, Sebire NJ, Timmer A, Turowski G, van der Voorn JP, van Lijnschoten I, Gordijn SJ. Sampling and definitions of placental lesions: Amsterdam Placental Workshop Group Consensus Statement. Arch Pathol Lab Med, 2016, 140(7):698–713. https://doi.org/10.5858/arpa.2015-0225-CC PMID: 27223167

[35] Romero R, Kim YM, Pacora P, Kim CJ, Benshalom-Tirosh N, Jaiman S, Bhatti G, Kim JS, Qureshi F, Jacques SM, Jung EJ, Yeo L, Panaitescu B, Maymon E, Hassan SS, Hsu CD, Erez O. The frequency and type of placental histologic lesions in term pregnancies with normal outcome. J Perinat Med, 2018, 46(6): 613–630. https://doi.org/10.1515/jpm-2018-0055 PMID: 30044764 PMCID: PMC6174692

[36] Novac MV, Niculescu M, Manolea MM, Dijmărescu AL, Iliescu DG, Novac MB, Rotaru LT, Stoenescu MF, Tabacu MC, Tudorache Ş, Busuioc CJ, Gheonea IA. Placental findings in pregnancies complicated with IUGR – histopathological and immunohistochemical analysis. Rom J Morphol Embryol, 2018, 59(3):715–720. PMID: 30534809

[37] Boldeanu L, Dijmărescu AL, Radu M, Siloşi CA, Popescu-Drigă MV, Poenariu IS, Siloşi I, Boldeanu MV, Novac MB, Novac LV. The role of mediating factors involved in angiogenesis during implantation. Rom J Morphol Embryol, 2020, 61(3):665–672. https://doi.org/10.47162/RJME.61.3.04 PMID: 33817707 PMCID: PMC8112745

[38] Jaiman S, Romero R, Bhatti G, Jung E, Gotsch F, Suksai M, Gallo DM, Chaiworapongsa T, Kadar N. The role of the placenta in spontaneous preterm labor and delivery with intact membranes. J Perinat Med, 2022, 50(5):553–566. https://doi.org/10.1515/jpm-2021-0681 PMID: 35246973 PMCID: PMC9189066
[39] Kaufmann P, Mayhew TM, Charnock-Jones DS. Aspects of human fetoplacental vasculogenesis and angiogenesis. II. Changes during normal pregnancy. Placenta, 2004, 25(2–3):114–126. https://doi.org/10.1016/j.placenta.2003.10.009 PMID: 14972444
[40] Junaid TO, Brownbill P, Chalmers N, Johnstone ED, Aplin JD. Fetoplacental vascular alterations associated with fetal growth restriction. Placenta, 2014, 35(10):808–815. https://doi.org/10.1016/j.placenta.2014.07.013 PMID: 25145956
[41] Tun WM, Yap CH, Saw SN, James JL, Clark AR. Differences in placental capillary shear stress in fetal growth restriction may affect endothelial cell function and vascular network formation. Sci Rep, 2019, 9(1):9876. https://doi.org/10.1038/s41598-019-46151-6 PMID: 31285454 PMCID: PMC6614400
[42] Berceanu C, Mehedinţu C, Berceanu S, Voicu NL, Brătilă E, Istrate-Ofiţeru AM, Navolan DB, Niculescu M, Szasz FA, Căpitănescu RG, Văduva CC. Morphological and ultrasound findings in multiple pregnancy placentation. Rom J Morphol Embryol, 2018, 59(2):435–453. PMID: 30173248
[43] Bărbălan A, Nicolaescu AC, Măgăran AV, Mercuţ R, Bălăşoiu M, Băncescu G, Şerbănescu MS, Lazăr OF, Săftoiu A. Immunohistochemistry predictive markers for primary colorectal cancer tumors: where are we and where are we going? Rom J Morphol Embryol, 2018, 59(1):29–42. PMID: 29940609
[44] Pleşea IE, Stoiculescu A, Şerbănescu M, Alexandru DO, Man M, Pop OT, Pleşea RM. Correlations between intratumoral vascular network and tumoral architecture in prostatic adenocarcinoma. Rom J Morphol Embryol, 2013, 54(2):299–308. PMID: 23771073
[45] Mitroi G, Pleşea RM, Pop OT, Ciovică DV, Şerbănescu MS, Alexandru DO, Stoiculescu A, Pleşea IE. Correlations between intratumoral interstitial fibrillary network and vascular network in Srigley patterns of prostate adenocarcinoma. Rom J Morphol Embryol, 2015, 56(4):1319–1328. PMID: 26743277
[46] Şerbănescu MS, Pleşea IE. A hardware approach for histological and histopathological digital image stain normalization. Rom J Morphol Embryol, 2015, 56(2 Suppl):735–741. PMID: 26429166
[47] Pleşea RM, Şerbănescu MS, Ciovică DV, Roşu GC, Moldovan VT, Bungărdean RM, Popescu NA, Pleşea IE. The study of tumor architecture components in prostate adenocarcinoma using fractal dimension analysis. Rom J Morphol Embryol, 2019, 60(2):501–519. PMID: 31658324
[48] Şerbănescu MS, Manea NC, Streba L, Belciug S, Pleşea IE, Pirici I, Bungărdean RM, Pleşea RM. Automated Gleason grading of prostate cancer using transfer learning from general-purpose deep-learning networks. Rom J Morphol Embryol, 2020, 61(1):149–155. https://doi.org/10.47162/RJME.61.1.17 PMID: 32747906 PMCID: PMC7728132
[49] Şerbănescu MS, Oancea CN, Streba CT, Pleşea IE, Pirici D, Streba L, Pleşea RM. Agreement of two pre-trained deep-learning neural networks built with transfer learning with six pathologists on 6000 patches of prostate cancer from Gleason2019 Challenge. Rom J Morphol Embryol, 2020, 61(2):513–519. https://doi.org/10.47162/RJME.61.2.21 PMID: 33544803 PMCID: PMC7864291

Corresponding authors

Anca-Maria Istrate-Ofiţeru, MD, PhD, Department of Histology, University of Medicine and Pharmacy of Craiova, 2 Petru Rareş Street, 200349 Craiova, Dolj County, Romania; Phone +40764–836 619, e-mail: ancaofiteru92@yahoo.com

Marius Bogdan Novac, Associate Professor, MD, PhD, Department of Anesthesiology and Intensive Care, University of Medicine and Pharmacy of Craiova, 2 Petru Rareş Street, 200349 Craiova, Dolj County, Romania; Phone +40744–278 405, e-mail: mariusnovac2005@yahoo.com

Received: May 23, 2022

Accepted: October 18, 2022